JACS
JOURNAL OF THE AMERICAN CHEMICAL SOCIETY
Communication
pubs.acs.org/JACS

Nonfluorescent Quenchers To Correlate Single-Molecule Conformational and Compositional Dynamics

Jin Chen,[†,‡] Albert Tsai,[†,‡] Alexey Petrov,[‡] and Joseph D. Puglisi[‡,*]

[†]Department of Applied Physics, Stanford University, Stanford, California 94305-4090, United States
[‡]Department of Structural Biology, Stanford University School of Medicine, Stanford, California 94305-5126, United States

Supporting Information

ABSTRACT: Single-molecule Förster resonance energy transfer (smFRET) is a powerful method for studying the conformational dynamics of a biomolecule in real-time. However, studying how interacting ligands correlate with and regulate the conformational dynamics of the biomolecule is extremely challenging because of the availability of a limited number of fluorescent dyes with both high quantum yield and minimal spectral overlap. Here we report the use of a nonfluorescent quencher (Black Hole Quencher, BHQ) as an acceptor for smFRET. Using a Cy3/BHQ pair, we can accurately follow conformational changes of the ribosome during elongation in real time. We demonstrate the application of single-color FRET to correlate the conformational dynamics of the ribosome with the compositional dynamics of tRNA. We use the normal Cy5 FRET acceptor to observe arrival of a fluorescently labeled tRNA with a concomitant transition of the ribosome from the locked to the unlocked conformation. Our results illustrate the potential of nonfluorescent quenchers in single-molecule correlation studies.

Single-molecule Förster resonance energy transfer (smFRET) is a powerful technique for studying biomolecular dynamics and interactions, providing conformational information regarding the system that is free from ensemble averaging. smFRET studies on transcription, translation, replication, recombination, RNA folding, and protein folding have revealed many rare, transient interactions and conformational subpopulations that are undetectable by bulk biochemical methods.[1−4] Recent single-molecule studies on translation allowed us to follow in real-time the ribosome conformation and transfer RNA (tRNA) dynamics.[5−13]

The efficiency of FRET between two fluorescent dye molecules (termed the donor and acceptor) depends strongly on the distance between the two molecules.[14] The energy transfer efficiency is given by

$$E = \frac{1}{1 + (r/R_0)^6} \tag{1}$$

where r is the interdye distance and R_0 is the Förster radius, defined as the interdye distance at which the FRET efficiency is 0.5.[15]

The Cy3/Cy5 dye pair is commonly employed in single-molecule systems. In an smFRET experiment, Cy3 (the donor) is excited with a 532 nm laser, and the energy is transferred to a nearby Cy5 (the acceptor), which then fluoresces in the red region of the spectrum. Because FRET alters the time-averaged fluorescence intensities of the donor and acceptor, the FRET efficiency can be simply calculated as

$$E = \frac{I_{Cy5}}{I_{Cy3} + I_{Cy5}} \tag{2}$$

The intensities used here have to be corrected for detection efficiencies, quantum yields, and background.

Even though smFRET reports on the conformational dynamics in real time with angstrom resolution, how these conformational dynamics correlate with the interactions of other compositions and ligands remains invisible. However, the small number of dyes suitable for single-molecule fluorescence hinders studies of such multicomponent systems by limiting the number of components that can be observed simultaneously. Another issue is that the photophysical behavior of acceptor dyes in FRET is often suboptimal, marred by short photobleaching times and long-lived nonfluorescent dark states. Also, the concentration of fluorescent acceptors in solution often cannot exceed 50 nM in fluorescence microscopy because of excessive background (due to cross-talk from donor excitation), hampering the investigation of many biological systems.

Here we report the use of a nonfluorescent quencher as an acceptor in FRET, thus mitigating the aforementioned problems. We replaced the acceptor dye Cy5 with the nonradiative acceptor Black Hole Quencher (BHQ-2; Figure 1a). The energy transferred from the donor dye to BHQ is released as heat instead of photons. By measuring the quenched intensity of the donor and comparing it with the unquenched intensity, we can calculate the single-dye FRET efficiency as

$$E = 1 - \frac{I_{Cy3}}{I_{Cy3,max}} \tag{3}$$

Using BHQ as the nonfluorescent FRET acceptor lacks the traditional anticorrelated intensity signal of the acceptor dye, but conformational information can still be extracted by examining the donor dye signal. This approach has several advantages. Most importantly, the use of BHQ frees the spectral region of the acceptor dye for labeling of other components of the system in multiplexed experiments. The use

Received: January 6, 2012
Published: March 19, 2012

 © 2012 American Chemical Society

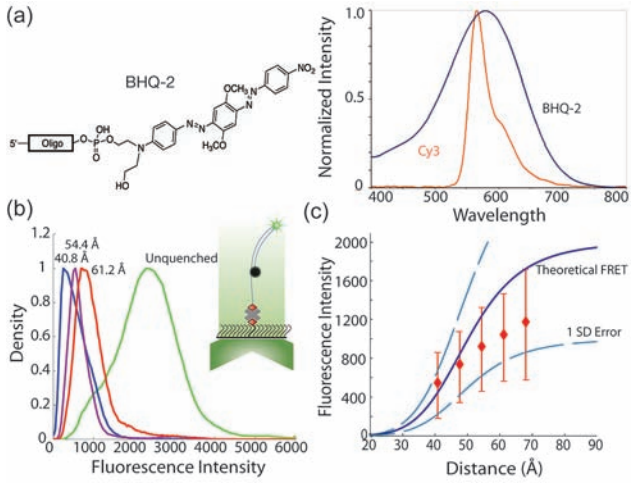

Figure 1. (a) (left) Chemical structure of BHQ-2 conjugated to an oligonucleotide. (right) The emission spectrum of Cy3 and the absorption spectrum of BHQ-2 show a large spectral overlap, enabling efficient energy transfer during FRET. (b) Intensity histogram of doubly labeled oligonucleotides with varying interdye distance between Cy3 and BHQ. (c) Mean Cy3 fluorescence intensity as a function of interdye distance, along with the theoretical FRET curve. Error bars represent 1 standard deviation. The mean intensity increases with increasing interdye distance, following the theoretical FRET curve within 1 standard deviation of error (resulting from the error in estimating I_{max} when calculating the fluorescence intensity from the FRET efficiency).

of BHQ further eliminates the poor behavior of the acceptor fluorescence, extending the observation time by removing the problem of photobleaching of the acceptor dye (Supplementary Figure 1 in the Supporting Information). The high spectral overlap between Cy3 and BHQ results in efficient energy transfer for FRET[16] (Figure 1a). Since BHQ itself is not fluorescent, the background noise is reduced, resulting in an increased signal-to-noise ratio at high concentrations of BHQ-labeled molecules. We demonstrated the utility of FRET with nonfluorescent quenchers for single-molecule dynamics and time-correlation measurements by observing conformational changes of the ribosome during translation in real time.

Previous work on nonfluorescent quenchers has shown their applications in a wide variety of systems. Schwartz and Quake[17] labeled opposite ends of a DNA hairpin with Cy3 and BHQ-2 to measure the replication through the hairpin by a DNA polymerase. Takada et al.[18] employed a TAMRA/BHQ system to investigate DNA hole transfer. Other work has also demonstrated the use of nonfluorescent quenchers in FRET assays and microscopy.[19−22] However, in this work, we demonstrate the use of BHQ to correlate the conformational dynamics of a biomolecule of interest with the interactions of other factors and ligands. This is of particular importance since the conformational dynamics of a biomolecule are often regulated through the interactions with other ligands.

The behavior of the donor dye/BHQ pair was first characterized by using oligonucleotide standards with varying distances between Cy3 and BHQ. We measured the Cy3 intensity of five duplex oligonucleotides with increasing distances between Cy3 and BHQ-2 ranging from 41 to 68 Å, assuming a B-form DNA conformation with a rise of 3.4 Å per base pair. A 5′-biotinylated and 3′-Cy3-labeled oligonucleotide was annealed to a series of 3′-BHQ-labeled oligonucleotides of varying length, providing a defined set of FRET distances between Cy3 and BHQ. The duplexes were immobilized on biotin−PEG-covered quartz surfaces through a neutravidin−biotin interaction and imaged using a prism-based total internal reflection fluorescence (TIRF) microscope with 532 nm excitation at 100 ms exposure time per frame.[5]

We observed the expected decrease in the Cy3 emission intensity as the interdye distance decreased, in excellent agreement with the theoretical FRET trace (Figure 1c), which was calculated using R_0 = 50.2 Å for Cy3/BHQ.[17] These results confirm that the Cy3/BHQ system works as a one-color FRET pair for single-molecule experiments with the expected quenching efficiencies.

Having shown that BHQ works as expected in static systems, we next characterized BHQ in a system with dynamic conformational changes, where most of the potential applications of BHQ lie. We characterized the behavior of the donor/BHQ pair using ratcheting *Escherichia coli* ribosomes that were site-specifically labeled with fluorescent dyes on the 30S and 50S subunits at positions that result in intersubunit FRET, a system that has been well-characterized previously.[5,23]

Cy3-labeled 30S preinitiation complexes (PICs) containing fMet-tRNA^{fMet} were immobilized through biotinylated messenger RNA (mRNA) on a poly(ethylene glycol) (PEG)-derivatized quartz surface. The 6(FK) mRNA contained the 5′ untranslated region (UTR) and the Shine−Dalgarno sequence from phage T4 gene 32, followed by six alternating Phe and Lys codons, a UAA stop codon, and four additional Phe codons. BHQ-labeled 50S subunits, the elongator ternary complex (TC) aa-tRNA·EF-Tu·GTP, elongation factor G (EF-G), and IF2 were delivered to the surface (Figure 2a). Initiation occurred when IF2-mediated 50S subunits joined to 30S

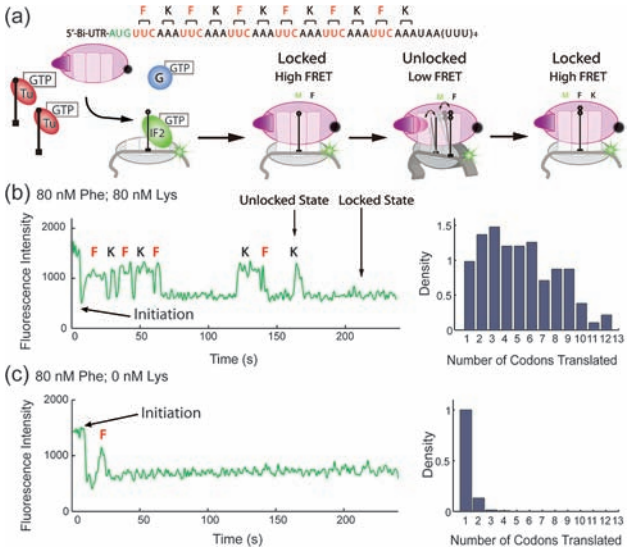

Figure 2. (a) Schematic illustrating the delivery of a BHQ-labeled 50S subunit with EF-G and ternary complex to a preassembled PIC immobilized on PEG-covered quartz surface. (b) (left) Representative time trace of the fluorescence intensity for an elongating ribosome translating mRNA 6(FK) (alternating Phe and Lys). (right) Histogram of the normalized number of elongation cycles observed for single ribosomes. (c) Representative time trace and corresponding histogram for an elongating ribosome translating 6(FK) without Lys tRNA. Translation stalled after the first codon. The small number of additional events beyond the first codon shown in the histogram are likely due to statistical errors in the identification of transitions by our analytical method.

subunits containing an initiator tRNA. The fluorescence intensity of Cy3 dropped upon assembly of the 70S complex during initiation as Cy3 was quenched by BHQ. During elongation, the fluorescence intensity alternated between high- and low-intensity states, which is consistent with the locking and unlocking of the ribosome upon translocation (Figure 2b). The high-intensity state (similar to the low-FRET state for Cy3/Cy5 FRET) corresponds to the unlocked conformation, and the low-intensity state corresponds to the locked conformation of the ribosome. Each cycle of low−high−low intensity states represents one round of elongation, as confirmed previously.[5] We calculated the FRET efficiency of the two states using eq 3.

Using the intensity before 50S subunit joining as I_{max} gives FRET efficiencies of ∼0.30 and ∼0.49 for the two states (Supplementary Figure 1). Given the R_0 of Cy3 and BHQ (50.2 Å), the Cy3/BHQ FRET efficiencies match well with theoretical calculations (Supplementary Figure 4). Thus, we were able to use BHQ to observe in real time the subunit joining and ribosomal conformational changes that occur during translation initiation and elongation.

Cy3/BHQ-labeled ribosomes were next used to follow the ribosome dynamics through multiple cycles of elongation. In the presence of Phe and Lys TCs (80 nM each) and EF-G, we observed ribosomes translating the entire 6(FK) mRNA (Figure 2b). The numbers of observed elongation cycles for ∼300 ribosomes are shown as histograms in Figure 2c,d. The main challenge for observation of all of the elongation cycles was fluorophore photobleaching. Withholding Lys tRNA TC correctly prevented the ribosome from proceeding beyond the first codon (Figure 2c).

To test whether our measured elongation rates depended properly on the TC and EF-G concentrations as previously reported,[5] we varied their concentrations. At 160 nM Phe TC and Lys TC but 80 nM EF-G, the apparent translation efficiency was higher than at 80 nM TC and 80 nM EF-G (Figure 3a), which is attributable to a higher elongation rate that results in translation of more codons before photobleaching of Cy3. The mean lifetimes of the two elongation states were determined by fitting the lifetimes to single-exponential distributions. Doubling the concentration of TC from 80 to 160 nM decreased the lifetime of the high-FRET state, corresponding to the locked conformation of the ribosome waiting for peptide bond formation (Figure 3c). The lifetime of the low-FRET state (the unlocked conformation of the ribosome waiting to translocate) did not change, as it depends on the concentration of EF-G (Figure 3d). Moreover, the rate of 50S subunit joining depends only on the concentration of the 50S subunit and not on the TC concentration (Supplementary Figure 3). Using Cy3- and BHQ-labeled ribosomes and our statistical analytical methods, we were able to identify accurately all of the ratcheting signals and to calculate mean lifetimes that agreed well with previous reports.[5] This shows that BHQ is effective as a nonfluorescent FRET acceptor for studying conformational dynamics.

We next extended the Cy3/BHQ FRET system by exploiting the vacant Cy5 spectral region, reintroducing Cy5 as a reporter for another molecule rather than as a Cy3 FRET acceptor. To improve our signal under dual illumination at 532 and 647 nm, we replaced the Cy3 fluorophore used to label the 30S subunit with Cy3B, which has an increased quantum yield. The FRET distributions and lifetimes for ribosomes labeled with Cy3B were identical to those obtained for Cy3-labeled ribosomes,

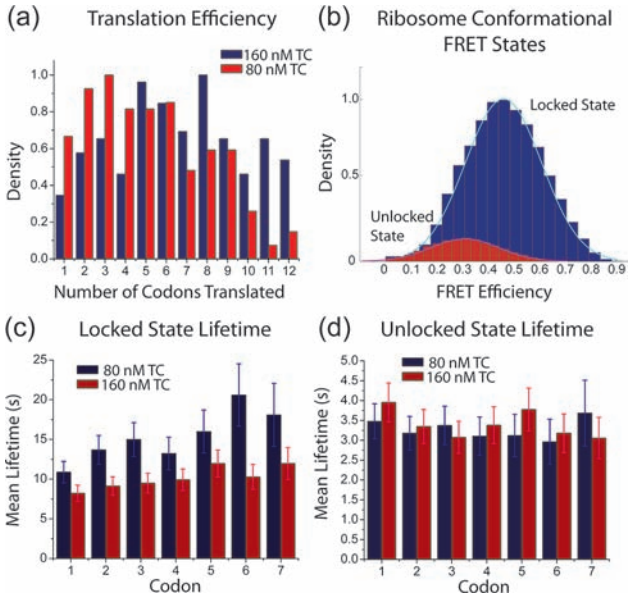

Figure 3. (a) Comparison histogram of apparent translation efficiencies at 80 nM TC (red) and 160 nM TC (blue). At higher [TC], the apparent translation efficiency is higher. (b) FRET efficiencies of the two conformational states, with means of 0.3 for the unlocked state and 0.49 for the locked state. (c) Mean lifetime of the locked state, which decreases as [TC] is increased. (d) Mean lifetime of unlocked state, which is not dependent on [TC].

except that their FRET efficiencies were shifted to higher values (∼0.4 and ∼0.6) (Supplementary Figure 5). From this, we calculated that R_0 for Cy3B and BHQ is ∼54 Å. As a result of the increased brightness of Cy3B and the higher signal-to-noise ratio (3.43 compared with 1.93 for Cy3), we could shorten the exposure time for data collection to 25 ms from the original 100 ms. This permitted the TC and EF-G concentrations to be increased to 200 and 500 nM, respectively, which approach the concentrations found in vivo. Under these conditions, we were able to identify accurately the ratcheting signals, obtaining lifetimes that matched the expected values (Supplementary Figure 6).

We followed the translation of the 6(FK) mRNA in the presence of Phe-(Cy5)tRNA^{Phe} and unlabeled Lys-tRNA^{Lys} to correlate the compositional signals of the arrival of tRNAs with the conformational dynamics of Cy3B/BHQ-labeled ribosomes. Arrival of a Phe-tRNA^{Phe}, shown as a red fluorescent pulse, is concomitant with the transition from low to high donor intensity of the ratcheting signal but sensitive to the position of the ribosome on the mRNA (Figure 4a). Postsynchronizing the ribosome conformational signals and the normalized red fluorescent pulses to the first and second high-to-low FRET transitions (low-to-high intensity transition) revealed that Phe-(Cy5)tRNA^{Phe} arrived only in the first FRET transition, consistent with the mRNA sequence. Within the time resolution of this measurement (100 ms), the arrival of Phe-(Cy5)tRNA^{Phe} occurred simultaneously with ribosome unlocking.

The observed mean Cy5 tRNA lifetime of 20.8 s (Supplementary Figure 7) and a signal-to-noise ratio of 1.59 (compared with the mean lifetime of <4 s and signal-to-noise ratio of <1.0 for Cy2)[5] allowed the arrival and departure of tRNAs to be followed. Our tRNA correlation experiment showed that tRNA^{Phe} arrival to the ribosome and peptide bond

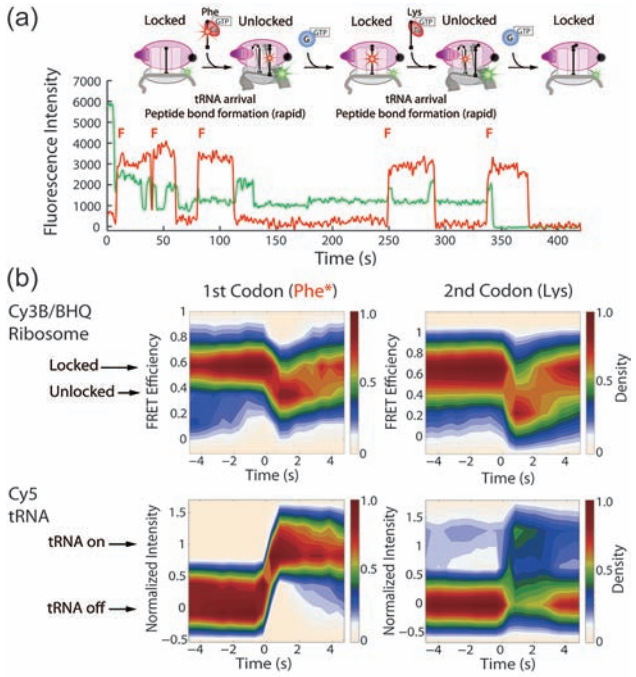

Figure 4. (a) Representative time trace of a correlation experiment, with the green trace (Cy3B) showing the ribosome locking and unlocking during elongation and the red trace (Cy5) showing the arrival and departure of Phe-tRNA^{Phe}. (b) Postsynchronized time traces of the arrival of Phe-(Cy5)tRNA^{Phe} and the conformation change of the ribosome from the locked to the unlocked state. The arrival of tRNA is directly correlated with the unlocking of the ribosome. The unlocking of the ribosome at the second codon is not correlated with a Cy5 pulse, consistent with the mRNA sequence.

formation are correlated with conformational changes of the ribosomal subunits, consistent with previous findings.[9−11] tRNA^{Phe} arrival and selection leads to the simultaneous unlocking of the ribosomal subunit. This tRNA then transits through the ribosome, passing from the A/P hybrid state into the P site upon one round of translocation. A subsequent tRNA^{Lys} then arrives, placing the tRNA^{Phe} in the P/E hybrid state. The final round of translocation, driven by EF-G, causes the locking of the ribosome and release of tRNA^{Phe} from the E site. With this signal, we were able to follow the ribosome in real time as it transitioned between the locked and unlocked conformations concurrent with tRNA transits. This method can be extended to other translation factors to study the correlation between the ribosomal conformational changes and these factors, or even to other biomolecular systems.

In summary, this study shows the promise of nonfluorescent FRET acceptors for correlating single-molecule conformational and compositional dynamics. We have used Cy3 (or Cy3B)-labeled 30S ribosomal subunits with BHQ-labeled 50S subunits to observe translation initiation and elongation in real time with single-codon resolution, and our results are comparable to previous data obtained using Cy3/Cy5 FRET. By the use of BHQ as the FRET acceptor, additional spectral channels are freed for multiplexed single-molecule experiments and correlation studies. This allows the study of not only the conformational dynamics but also the interactions among multiple biomolecules and how they regulate the conformation. BHQ thus provides a powerful way to investigate the correlated dynamics of different factors that were not previously accessible.

■ ASSOCIATED CONTENT

Supporting Information

Supplementary figures, information, and data. This material is available free of charge via the Internet at http://pubs.acs.org.

■ AUTHOR INFORMATION

Corresponding Author

puglisi@stanford.edu

Notes

The authors declare no competing financial interest.

■ ACKNOWLEDGMENTS

We thank Seán O'Leary (Stanford), Guy Kornberg (Stanford), and Thomas Noriega (UCSF) for valuable discussions. This work was funded by NIH Grant GM51266.

■ REFERENCES

(1) Joo, C.; Balci, H.; Ishitsuka, Y.; Buranachai, C.; Ha, T. *Annu. Rev. Biochem.* **2008**, *77*, 51.
(2) Weiss, S. *Science* **1999**, *283*, 1676.
(3) Weiss, S. *Nat. Struct. Biol.* **2000**, *7*, 724.
(4) Tinoco, I. Jr.; Gonzalez, R. L. Jr. *Genes Dev.* **2011**, *25*, 1205.
(5) Aitken, C. E.; Puglisi, J. D. *Nat. Struct. Mol. Biol.* **2010**, *17*, 793.
(6) Blanchard, S. C.; Gonzalez, R. L.; Kim, H. D.; Chu, S.; Puglisi, J. D. *Nat. Struct. Mol. Biol.* **2004**, *11*, 1008.
(7) Blanchard, S. C.; Kim, H. D.; Gonzalez, R. L. Jr.; Puglisi, J. D.; Chu, S. *Proc. Natl. Acad. Sci. U.S.A.* **2004**, *101*, 12893.
(8) Cornish, P. V.; Ermolenko, D. N.; Noller, H. F.; Ha, T. *Mol. Cell* **2008**, *30*, 578.
(9) Fei, J.; Bronson, J. E.; Hofman, J. M.; Srinivas, R. L.; Wiggins, C. H.; Gonzalez, R. L. Jr. *Proc. Natl. Acad. Sci. U.S.A.* **2009**, *106*, 15702.
(10) Fei, J.; Kosuri, P.; MacDougall, D. D.; Gonzalez, R. L. Jr. *Mol. Cell* **2008**, *30*, 348.
(11) Marshall, R. A.; Dorywalska, M.; Puglisi, J. D. *Proc. Natl. Acad. Sci. U.S.A.* **2008**, *105*, 15364.
(12) Uemura, S.; Aitken, C. E.; Korlach, J.; Flusberg, B. A.; Turner, S. W.; Puglisi, J. D. *Nature* **2010**, *464*, 1012.
(13) Wen, J. D.; Lancaster, L.; Hodges, C.; Zeri, A. C.; Yoshimura, S. H.; Noller, H. F.; Bustamante, C.; Tinoco, I. *Nature* **2008**, *452*, 598.
(14) Roy, R.; Hohng, S.; Ha, T. *Nat. Methods* **2008**, *5*, 507.
(15) Lakowicz, J. R. *Principles of Fluorescence Spectroscopy*, 3rd ed.; Springer: New York, 2006.
(16) Marras, S. A.; Kramer, F. R.; Tyagi, S. *Nucleic Acids Res.* **2002**, *30*, e122.
(17) Schwartz, J. J.; Quake, S. R. *Proc. Natl. Acad. Sci. U.S.A.* **2009**, *106*, 20294.
(18) Takada, T.; Takeda, Y.; Fujitsuka, M.; Majima, T. *J. Am. Chem. Soc.* **2009**, *131*, 6656.
(19) Orte, A.; Clarke, R. W.; Klenerman, D. *Anal. Chem.* **2008**, *80*, 8389.
(20) Youn, H. J.; Terpetschnig, E.; Szmacinski, H.; Lakowicz, J. R. *Anal. Biochem.* **1995**, *232*, 24.
(21) Tahmassebi, D. C.; Millar, D. P. *Biochem. Biophys. Res. Commun.* **2009**, *380*, 277.
(22) Ganesan, S.; Ameer-Beg, S. M.; Ng, T. T.; Vojnovic, B.; Wouters, F. S. *Proc. Natl. Acad. Sci. U.S.A.* **2006**, *103*, 4089.
(23) Dorywalska, M.; Blanchard, S. C.; Gonzalez, R. L.; Kim, H. D.; Chu, S.; Puglisi, J. D. *Nucleic Acids Res.* **2005**, *33*, 182.